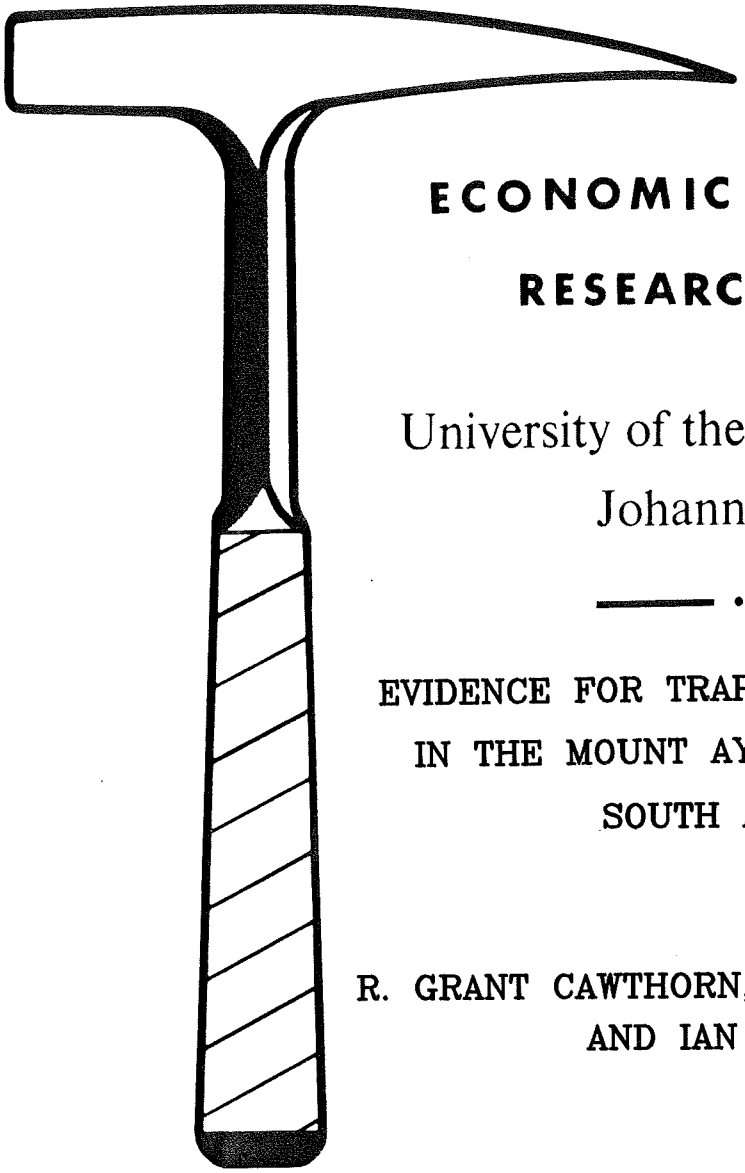

ECONOMIC GEOLOGY

RESEARCH UNIT

University of the Witwatersrand

Johannesburg

EVIDENCE FOR TRAPPED LIQUID SHIFT IN THE MOUNT AYLIFF INTRUSION, SOUTH AFRICA

R. GRANT CAWTHORN, BERNHARD K. SANDER AND IAN M. JONES

INFORMATION CIRCULAR No. 239

UNIVERSITY OF THE WITWATERSRAND
JOHANNESBURG

EVIDENCE FOR TRAPPED LIQUID SHIFT IN THE MOUNT AYLIFF INTRUSION, SOUTH AFRICA

R. GRANT CAWTHORN, BERNHARD K. SANDER and IAN M. JONES

(Department of Geology, University of the Witwatersrand, P.O. Wits 2050, South Africa)

ECONOMIC GEOLOGY RESEARCH UNIT
INFORMATION CIRCULAR No. 239

September, 1991

EVIDENCE FOR TRAPPED LIQUID SHIFT IN THE MOUNT AYLIFF INTRUSION, SOUTH AFRICA

ABSTRACT

The consequence of postcumulus trapped liquid shift (Barnes, 1986) is that it produces cumulate minerals in a layered complex which appear more differentiated than the original primary cumulus compositions. Independent evidence for this effect is presented here using data from the basal, picritic facies of the Mount Ayliff Intrusion. The existence of cumulates with a wide range of olivine:interstitial liquid proportions produces a suite of rocks which define a tight linear trend on a binary whole-rock plot of MgO versus FeO. Extrapolation of this trend constrains the composition of the primary cumulus olivine to be in the range Fo_{84-86}. Analyses of the olivine present in these samples give compositions of Fo_{83-77}. The magnitude of the discrepancy between the theoretical and observed olivine compositions correlates directly with the proportion of interstitial liquid. These observations are quantitatively predicted by the trapped liquid shift model. Specifically, they also argue against general migration of residual liquid relative to the cumulus minerals. Trapped liquid shift is documented over a vertical interval of 60m. It can be demonstrated to have occurred in rocks lying only 1m above the basal contact and hence must be a comparatively rapid process; certainly fast enough for this process to be of significance in postcumulus processes in large layered intrusions. An MgO versus FeO variation diagram for a suite of olivine cumulate rocks and their observed olivine compositions can lead to the incorrect estimation of the parental magma composition if the trapped liquid effect is ignored.

oOo

EVIDENCE FOR TRAPPED LIQUID SHIFT IN THE MOUNT AYLIFF INTRUSION, SOUTH AFRICA

CONTENTS

oOo

Published by the Economic Geology Research Unit
University of the Witwatersrand
1 Jan Smuts Avenue
Johannesburg 2001
South Africa

ISBN 1 874856 45 1

EVIDENCE FOR TRAPPED LIQUID SHIFT IN THE MOUNT AYLIFF INTRUSION, SOUTH AFRICA

INTRODUCTION

Postcumulus processes undoubtedly affect the final whole rock and mineral compositions of rocks in layered complexes. However, the extent of such reactions is difficult to quantify because original cumulus mineral compositions and primary porosity are usually not independently determinable. Various scenarios have been postulated for the reaction between cumulus minerals and intercumulus liquid. It has also been debated whether the intercumulus liquid is trapped or migrates relative to the cumulus minerals which formed from it. Irvine (1978, 1980) suggested that residual liquid might filter upwards and react with minerals not in equilibrium with the liquid. Tait et al. (1984) considered the density of differentiating liquids and suggested that at certain levels in an intrusion the residual liquid would sink and react with earlier-formed minerals. Barnes (1986) made quantitative calculations of the effect on cumulus mineral compositions reacting with varying proportions of intercumulus liquid. His model assumed that the liquid remained trapped relative to the cumulus crystals; and termed the change in mineral composition the "trapped liquid shift". These models may be complementary with different processes operative in different intrusions or at different stratigraphic levels in the same intrusion.

Barnes (1986) presented several examples in layered complexes where the patterns of mineral compositions in short vertical sections did not fit with simple fractional crystallization of a single liquid, but were consistent with a superimposed trapped liquid shift. He specifically referred to the Insizwa lobe of the Mount Ayliff Intrusion and suggested that the apparent inverse upward differentiation in olivine compositions near the base of the intrusion could be explained by reaction with progressively decreasing proportions of trapped liquid. Paktunc (1987) and Chalowku and Grant (1987) have also argued that changes in primary composition have occurred, based on correlation between mode and composition of olivine. Here, the writers present whole rock data from several profiles through the Mount Ayliff Intrusion which permit an independent determination of the cumulus olivine composition. This can then be compared with the actual minerals present in the rock.

THEORY

Barnes (1986) discussed the principle behind re-equilibration of cumulus phases and residual liquid, and showed how the size of the trapped liquid shift relates to the proportion of cumulus phase present. The authors use an oxide variation diagram to illustrate this process and then present data to test the extent of this effect. Olivine accumulation is the simplest situation to represent geometrically (Fig. 1) as the olivine compositions can be related to that of the liquid by the equations of Roeder and Emslie (1970). Liquid L^C crystallizes olivine F^C. A package of liquid plus crystals, of bulk composition B, then undergoes re-equilibration at temperatures between the liquidus and solidus. The composition of the olivine is depleted in Fo and the residual liquid decreases in total MgO and FeO. The effect is that the tie-line joining

instantaneous liquid and cumulus crystal composition rotates (from L^CF^C to L^SF^S). If the interstitial liquid remains trapped rotation is pivotted about the bulk composition. (If the package contains a large proportion of olivine (B^1), the effect on the olivine composition will be small (tie-line L^1F^1). Conversely, if the package has a small proportion of olivine (B^2), the effect will be greater (L^2F^2).

In most layered complexes the proportion of trapped liquid does not vary greatly over small vertical intervals, and so a wide range of bulk compositions is rarely available for study. In the theoretical example of Figure 1 there is a large variation in the olivine:liquid proportions and so it is possible to determine the primary, cumulus composition of the olivine (F^C) by a construction line through all the bulk compositions (B^1-B^2). Hence, the observed composition (determined by analysis) can be compared with the original, primary composition (determined by construction). In this way, an independent test of the extent of the trapped liquid shift is available.

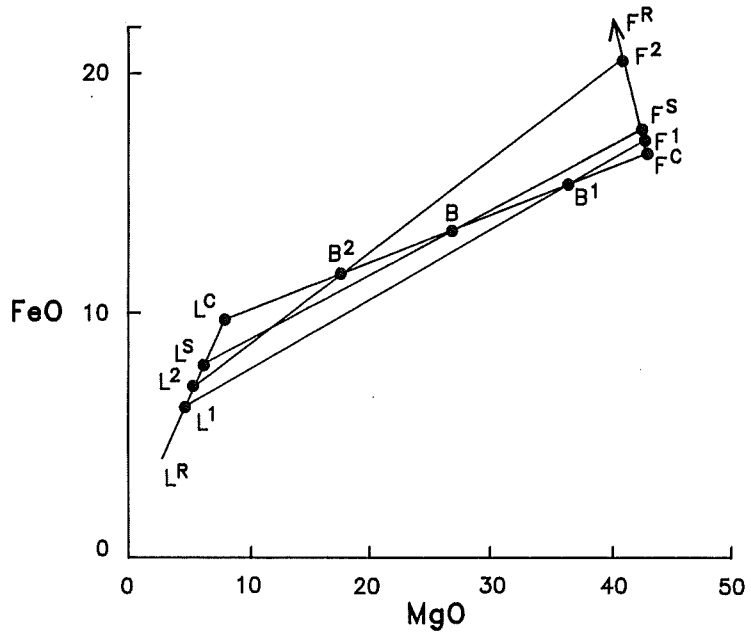

Figure 1: MgO versus FeO variation diagram illustrating the geometrical relations between liquid (L), olivine (F) and bulk rock (B) compositions. Parental liquid L^C crystallizes olivine F^C. Accumulation of that olivine into the liquid produces bulk rock compositions B, B^1, B^2 depending upon the proportions. Subsequent re-equilibration between interstitial liquid and olivine rotates the tie-lines, which must pivot about the whole rock composition. Thus, whole rock B^1 produces equilibrated olivine F^1 and a fictive liquid L^1, while B^2 produces olivine F^2 and fictive liquid L^2. Where there is minimal olivine present the liquid will change towards L^R and the olivine F^R. The original cumulus olivine F^C can be predicted by construction through B^2-B-B^1, but is not preserved in the rocks.

There are two restrictions and complications which limit the applicability of this model. If there is more than one cumulus silicate phase, then the bulk composition is constrained within a triangle, not

along a straight line; and precise prediction of primary compositions is not possible. If a long vertical section of cumulates is considered, the primary composition of the cumulus phase may change due to differentiation and the bulk compositions would no longer define a linear trend. This is shown in Figure 2, where a series of packages is produced from a differentiating liquid (L^1-L^3), such that the olivines range from F^1-F^3. In Figure 2 the bulk rocks (B^1-B^3) have a constant proportion of olivine:liquid of 2:1, but if they have random proportions they would scatter along their respective tie-lines and give an apparently meaningless distribution of points.

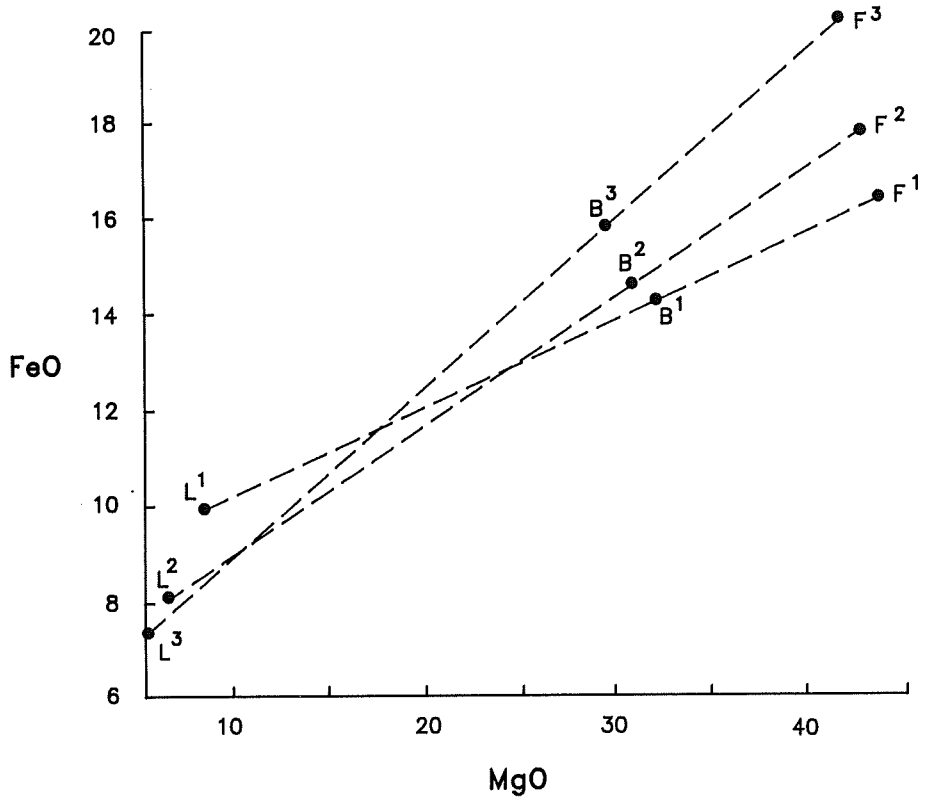

Figure 2: MgO versus FeO variation diagram illustrating the range of cumulates formed during differentiation. Liquid L^1 crystallizes olivine F^1 producing a bulk rock B^1. As the liquid differentiates it changes to L^2, the olivine to F^2, and the bulk rock to B^2. Each cumulate rock is arbitrarily shown containing 33% olivine.

MOUNT AYLIFF INTRUSION

The geology of this complex (Fig. 3) has been described in numerous papers (Scholtz, 1936; Lightfoot and Naldrett, 1984 ; Lightfoot et al., 1984, 1987 ; Cawthorn et al., 1985, 1986, 1988, 1991), and is not repeated here. At the base of the intrusion there is a discontinuous picrite horizon, which provides an opportunity to study the effect of olivine accumulation. There is generally an olivine gabbro below the picrite, reaching 15m at Waterfall Gorge (Lightfoot et al., 1984), but at Mount Evelyn it is less than 3m. The maximum thickness of picrite in exposed profiles is 300m, but most emphasis will be placed on the lowermost sequence in this paper.

GEOCHEMISTRY

The writers have taken eleven profiles through the picritic facies of the Tonti and Insizwa lobes of the intrusion (Fig. 3). Exposure permitting, whole rock analyses have been determined at typically 20 m intervals in the picrite, and at closer intervals in the underlying olivine gabbro. Representative data are presented in Table 1 and Figures 4 and 5. In some instances olivine has been analysed by electron microprobe (Cawthorn et al., 1986), but in most cases the olivine has been separated and analysed by XRF spectrometry. Multiple electron microprobe analyses and traverses across single grains of olivine have shown that the olivine is homogeneous (Cawthorn et al., 1986), and so direct comparison with the XRF data is possible. For the Waterfall Gorge section both electron microprobe (from Lightfoot et al., 1984) and XRF analyses (this study) agree.

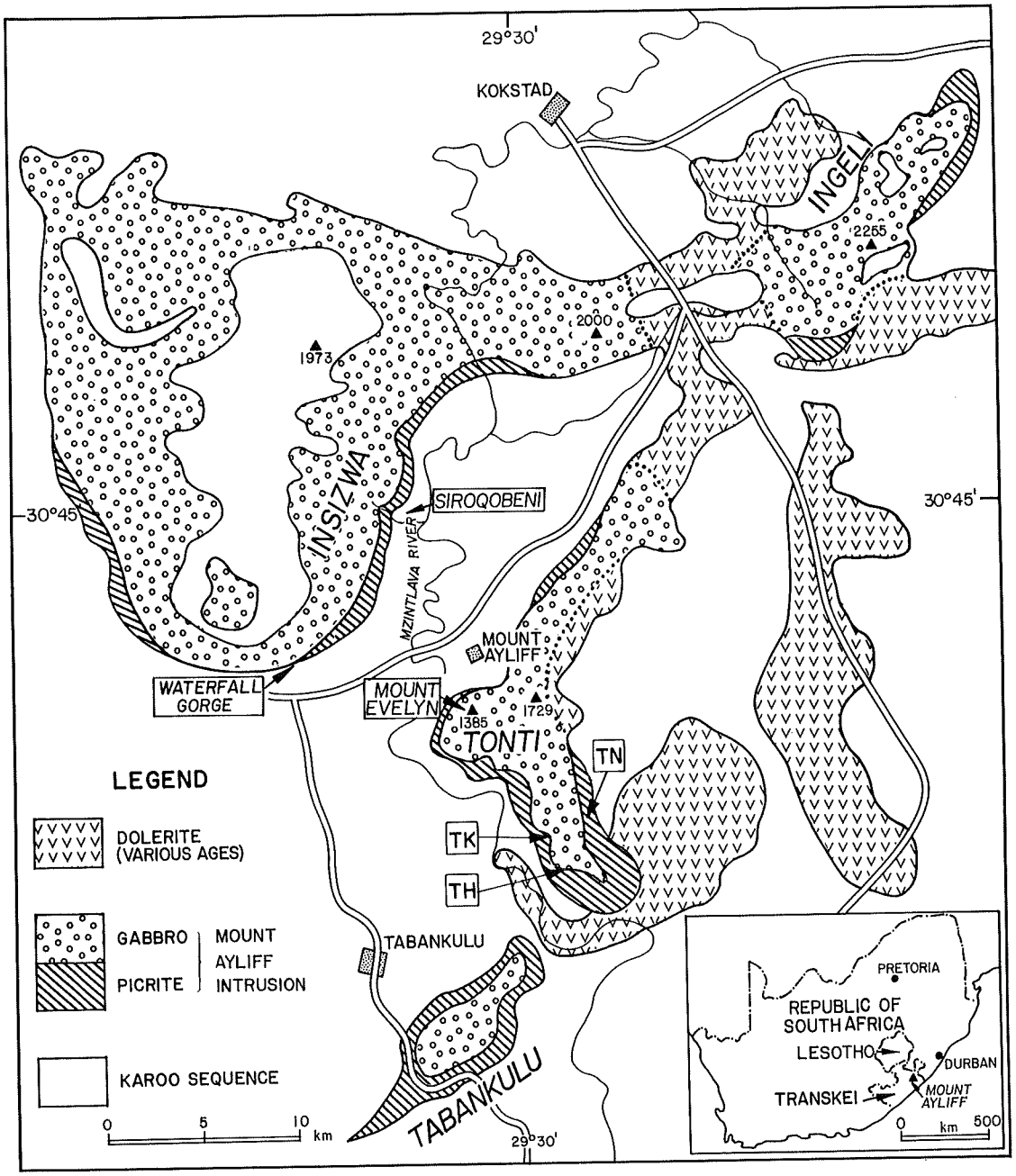

Figure 3: Simplified geological map of the Mount Ayliff Intrusion showing the locations of the profiles sampled through the picrite at Waterfall Gorge and Siroqobeni in the Insizwa lobe; and Mount Evelyn, TN, TH and TK in the Tonti lobe.

TABLE 1: Whole rock and olivine analyses from picrite of the Mount Ayliff Intrusion

Mount Evelyn profile - TONTI								
Sample	Pr21/1	Pr21/2	Pr21/3	Pr21/4	Pr21/5	Pr21/6	Pr21/7	Pr21/8
Height(m)	1	3	6	10	14	19	35	52
Whole Rock (weight percent)								
SiO_2	47.5	44.4	43.6	42.1	42.8	42.2	41.9	43.8
TiO_2	.71	.41	.30	.20	.25	.24	.15	.28
Al_2O_3	10.1	5.9	5.7	5.0	4.9	4.9	5.0	4.7
Fe_2O_3	11.8	14.3	14.5	14.4	14.5	14.6	15.1	16.0
MnO	.2	.2	.2	.2	.2	.2	.2	.2
MgO	19.5	29.9	31.7	33.3	34.4	33.2	34.2	32.8
CaO	6.8	3.7	3.4	3.1	3.0	3.0	2.9	3.4
Na_2O	1.78	1	.91	.81	.77	.77	.63	.74
K_2O	.49	.37	.25	.13	.16	.15	.07	.13
P_2O_5	.11	.07	.06	.05	.07	.05	.04	.06
Total	99.0	100.2	100.6	99.3	101.2	99.3	100.2	102.2
Trace elements (ppm)								
Ba	162	114	78	50	57	59	36	51
Rb	13	10	5	2	7	2	4	6
Sr	198	70	63	52	63	60	63	57
Y	24	14	9	7	8	8	6	8
Zr	72	35	20	11	39	35	27	34
Nb	6	0	0	1	2	1	0	2
Cu	113	121	130	155	81	157	114	103
Co	55	117	120	127	128	131	139	129
Ni	344	710	663	671	848	1298	514	405
Zn	87	98	96	92	94	92	91	105
V	228	198	170	171	129	161	116	123
Cr	1558	4128	4273	4027	5136	6542	4166	2873
S	920	1040	560	1710	700	1570	1580	1390
Olivine compositions (weight percent)								
Technique	XRF	Probe	XRF	Probe	Probe	Probe	XRF	XRF
SiO_2	39.9	38.8	37.5	39.1	39.3	39.2	38.5	37.9
TiO_2	.65	-	.77	-	-	-	.28	.42
Al_2O_3	1.6	.01	1.0	.02	.02	.02	1.1	.4
FeO*	18.1	17.6	17.3	16.1	15.9	15.7	16.3	18.7
MnO	.2	.2	.2	.2	.2	.2	.2	.2
MgO	36.9	43.3	40.2	44.5	44.7	44.8	41.2	40.6
CaO	1.0	.11	.4	.09	.10	.08	.5	.2
Total	98.3	100.3	97.3	100.1	100.4	100.1	98.1	98.5
Fo-Ol	78.5	81.4	80.5	83.1	83.4	83.5	81.8	79.5
Trace elements (ppm)								
Ni	900	930	860	610	1100	1300	610	510

Mbangweni profile - INSIZWA							
Sample	Pr12/1	Pr12/2	Pr12/3	Pr12/5	Pr12/6	Pr12/7	Pr12/8
Height(m)	.50	7	15	32	43	55	86
Whole Rock (weight percent)							
SiO_2	52.0	48.9	44.8	44.6	44.5	44.3	44.3
TiO_2	.77	.56	.37	.43	.32	.22	.27
Al_2O_3	12.6	9.8	5.3	6.7	4.2	4.9	3.9
Fe_2O_3	11.4	11.9	14.6	14.2	14.9	13.9	14.9
MnO	.2	.2	.2	.2	.2	.2	.2
MgO	10.4	19.7	28.4	28.3	30.5	31.8	32.2
CaO	9.7	7.1	4.3	4.3	4.1	4.5	3.9
Na_2O	1.84	1.57	1.07	1.22	.84	.74	.71
K_2O	.63	.53	.17	.26	.13	.09	.10
P_2O_5	.10	.10	.04	.08	.05	.04	.04
Total	99.7	100.4	99.2	100.2	99.8	100.6	100.6
Trace elements (ppm)							
Ba	171	145	78	99	59	36	40
Rb	17	15	6	11	4	5	4
Sr	99	76	76	92	51	60	49
Y	22	15	12	13	10	10	9
Zr	69	55	42	54	36	29	31
Nb	1	2	3	2	3	1	1
Cu	69	76	182	269	123	149	83
Co	41	72	111	121	124	124	128
Ni	153	455	831	946	894	1019	1084
Zn	89	84	91	95	110	83	96
V	254	187	138	134	141	99	115
Cr	566	1142	2482	2695	2566	2568	2225
S	550	550	1150	1580	870	940	1040
Olivine compositions (weight percent)							
SiO2	38.6	38.3	37.9	38.2	38.2	38.2	
TiO2	.36	.17	.37	.15	.09	.10	
Al2O3	.7	.4	.8	.2	.3	.2	
FeO*	20.5	18.9	18.5	18.4	16.2	17.4	
MnO	.3	.2	.2	.2	.2	.2	
MgO	38.1	42.1	41.2	42.7	44.2	42.4	
CaO	.6	.3	.4	.2	.3	.2	
Total	99.2	100.4	99.3	100.1	99.5	98.8	
Fo-Ol	76.8	79.9	79.9	80.5	83	81.3	
Trace elements (ppm)							
Ni	1200	1320	1450	1370	1470	1570	

Siroqbeni profile - INSIZWA								
Sample	Pr16/0	Pr16/1	Pr16/2	Pr16/3	Pr16/4	Pr16/5	Pr16/6	Pr16/7	Pr16/8
Height(m)	2	7	21	27	40	60	87	101	124
Whole Rock (weight percent)									
SiO_2	48.2	45.6	43.5	43.4	43.2	42.7	43.3	41.9	43.2
TiO_2	.65	.42	.27	.30	.30	.26	.35	.23	.27
Al_2O_3	10.1	7.8	5.1	5.3	4.9	5.0	5.2	5.2	5.1
Fe_2O_3	11.9	12.9	13.9	14.1	14.5	14.5	15.1	15.0	14.0
MnO	.2	.2	.2	.2	.2	.2	.2	.2	.2
MgO	20.0	25.9	32.9	31.6	32.4	33.8	31.4	32.5	33.7
CaO	6.5	5.1	3.3	3.5	3.3	3.3	3.5	3.5	3.4
Na_2O	1.75	1.39	.95	.92	.90	.86	2.21	.90	1
K_2O	.52	.29	.17	.17	.21	.16	.23	.09	.09
P_2O_5	.11	.07	.05	.05	.06	.05	.06	.04	.04
Total	99.9	99.8	100.3	99.5	100	100.8	101.5	99.7	101.0
Trace elements (ppm)									
Ba	154	95	62	61	68	60	70	46	78
Rb	19	11	11	7	11	9	5	6	8
Sr	126	93	61	63	64	63	61	62	68
Y	20	12	9	8	9	10	6	7	11
Zr	76	53	41	35	41	38	30	31	41
Nb	6	2	3	2	4	3	2	2	4
Cu	82	76	249	238	242	422	180	370	375
Co	72	94	128	115	125	134	127	140	137
Ni	593	862	1187	1078	1067	1494	1376	1325	1112
Zn	86	84	86	81	89	80	83	87	86
V	183	142	117	111	111	104	124	102	134
Cr	1806	2588	3254	3185	2970	2947	4825	3954	3844
S	730	650	1550	1550	1150	2170	850	1970	2700
Olivine compositions (weight percent)									
SiO_2	42.8	41.1	39.0	38.9	38.7	39.9	38.6	38.6	38.6
TiO_2	.56	.32	.37	.31	.28	.27	.17	.33	.27
Al_2O_3	1.8	1.8	.7	1.0	.9	.7	.5	.8	.3
FeO*	17.6	16.4	16.0	16.1	16.7	15.9	16.0	17.7	17.2
MnO	.2	.2	.2	.2	.2	.2	.3	.2	.3
MgO	34.8	38.1	41.8	40.2	41.8	42.1	43.0	40.8	41.9
CaO	2.2	1.5	.3	.6	.2	.4	.2	.3	.2
Total	100	99.5	98.5	97.4	98.8	99.4	98.7	98.7	98.7
Fo-Ol	77.9	80.6	82.3	81.6	81.7	82.5	82.7	80.5	81.3
Trace elements (ppm)									
Ni	1210	1370	1520	1590	1450	1910	1750	1670	1200

Plots of olivine compositions versus height have been presented by Cawthorn et al. (1986). Typically Fo increases upwards through the bottom 10-30m, and thereafter it either remains constant or decreases. The basal section with the largest range in whole-rock MgO contents is from the old mine adits at Waterfall Gorge (Lightfoot and Naldrett, 1984; Lightfoot et al., 1984; this study) and the data are shown in Figure 4. The olivine compositions become more forsteritic upwards over 20m from Fo_{77} to Fo_{81}. However, there is a small reversal in the trend at 5-8m. All incompatible trace elements, as exemplified by Zr in Figure 4, show a decrease upwards, reflecting a decreasing proportion of trapped liquid (see Lightfoot and Naldrett, 1984 for comparable plots for other incompatible trace and major elements). Again there is a slight reversal in the trend at 5-8m, identical to the olivine trend. The authors resampled this section in order to confirm the existence of this reversal, and our results are consistent with those from Lightfoot and Naldrett (1984). There was insufficient euhedral olivine in the samples below 5m for mineral separation and analysis in this study.

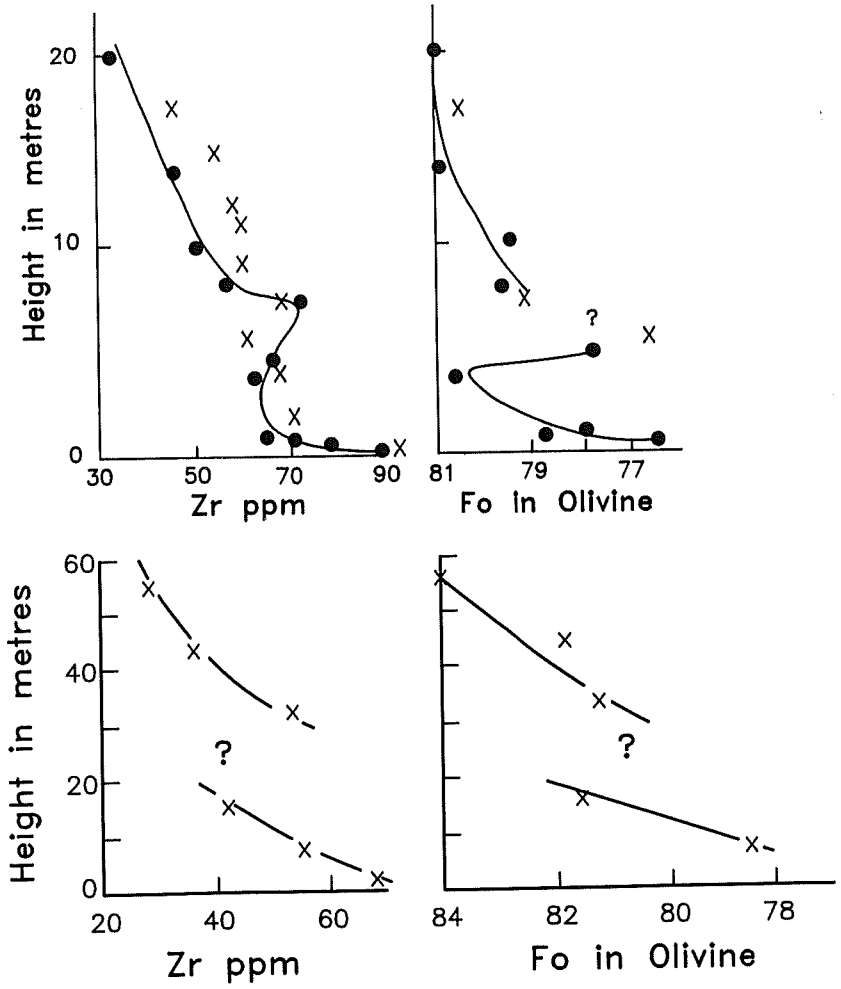

Figure 4: *Plot of whole rock Zr content and olivine composition versus height above the base of the intrusion at Waterfall Gorge (upper diagrams) and Mount Evelyn (lower diagrams). The circles are from the data of Lightfoot and Naldrett (1984) and Lightfoot et al. (1984) and the crosses from this study. The Zr profile shows a reversal in the general trend between 5-8m, which is probably also present in the olivine compositions but there are insufficient analyses in this crucial interval.*

A comparable, though less detailed section through the Mount Evelyn profile is also presented in Figure 4. This too shows a break in olivine and Zr trends, but at a greater height than in the Waterfall Gorge section.

MODELS FOR PRODUCING REVERSALS IN MINERAL COMPOSITIONS

Basal reversals in mineral compositions are not unusual in layered complexes and several mechanisms have been invoked to explain specific examples (Wilson et al., 1987). These hypotheses are discussed here in relation to the Mount Ayliff Intrusion.

A. Infiltration Metasomatism

Addition of less differentiated magma will cause a reversal in mineral compositions, which could be gradational if there is reaction with underlying, low density interstitial liquid (as observed in the Muskox Intrusion) (Irvine, 1980). However, in the present case, there are no cumulates to produce the infiltrating liquid underlying the suite of rocks showing an upward reversal in composition, and so this model cannot apply.

B. Addition into a Zoned Magma

Wilson et al. (1987) documented gradual reversals in mineral composition which are transgressive to the modal layering. Their model requires gradual intrusion of less differentiated magma into a zoned magma chamber, which was crystallizing on an inclined floor. In the case of the Mount Ayliff Intrusion, there are no pre-existing cumulates which could have generated a zoned magma chamber. The floor to the picrite unit may be inclined. This can be demonstrated from a consideration of the altitudes of the floor contact in each of the profiles studied. These range from 1068m at Siroqobeni, 1170m at Waterfall Gorge, to 1225m at Mbangweni in the Insizwa lobe; and from 878m in profile TK, 998m at TH, 1095m at TN to 1125m at Mount Evelyn in the Tonti lobe. Despite these vertical differences within individual lobes their basal olivine compositions are comparable. There is no change in mineral composition along the sloping floor in Mount Ayliff Intrusion as observed in the Fongen-Hyllingen Intrusion. Hence, there is no evidence for a zoned magma chamber at the stage of its crystallization being considered here, and so the model which applies for the Fongen-Hyllingen Intrusion is not appropriate in the Mount Ayliff Intrusion.

C. Supercooling and/or Rapid Cooling

Dynamic experimental studies, especially on lunar basalts (reviewed by Lofgren, 1980), have produced strongly zoned olivine crystals. This is the result of a combination of supercooling which causes a more iron-rich mineral to nucleate and continued growth of the crystal as the melt changes composition, although the former effect is minimal (Walker et al., 1976). This would produce a bulk olivine composition more iron-rich than the expected cumulus crystal. The combined effects only become significant at cooling rates greater than $2°C.h^{-1}$. Donaldson (1976) documented the morphology of olivine crystals as a function of cooling rate. At rates in excess of $2°C.h^{-1}$ crystals are no longer euhedral but become progressively more skeletal. As the olivine in the basal olivine gabbro and picrite is granular to tabular (Cawthorn et al., 1985) this precludes cooling rates sufficiently fast to produced more iron-rich olivine. Furthermore, cumulate rocks, with 20-50% olivine, could not be produced in a magma chamber

which is cooling at those rates.

While all the above mechanisms can and probably do occur in specific instances, they do not fit the observations on reverse differentiation of the olivine compositions at the base of the Mount Ayliff Intrusion.

TRAPPED LIQUID SHIFT MODEL

Typical whole rock data from Mount Ayliff are plotted in Figure 5. Before interpreting these in detail, it is necessary to discuss some minor recalculations of the data. Analyses by XRF are for total iron. Some Fe_2O_3 will be present. As these rocks are enriched in olivine the Fe_2O_3/FeO ratio will be much lower than for a basic liquid. The olivine contains more iron than the liquid (Fig. 1) and so for a typical rock with 50% cumulus olivine and 50% trapped liquid with a Fe_2O_3/FeO ratio of 0.1, the bulk ratio would be 0.04. Allowing for the effect of Fe_2O_3 would cause all the data points to move to lower FeO contents on Fig. 4, and would yield a more forsteritic olivine in the subsequent calculations. However, the exact figure for each sample cannot be aproximated, and for consistency no correction for Fe_2O_3 is applied here.

Chromite is also present as a cumulus phase. The typical proportion of chromite:olivine of 1.5:98.5 is calculated from the whole rock composition, first using the whole-rock MgO content to determine the proportion of olivine, and then the Cr content to determine the proportion of chromite. The calculation is reiterated to include the effects of MgO in chromite and Cr in olivine. However, as the MgO content of the chromite is about the same as that of the liquid (Cawthorn et al., 1991), and as the Cr contents of the olivine and liquid are extremely small compared to that of the chromite, reiteration has a negligible effect. Once the proportion of chromite has been determined, an amount of total FeO and MgO equivalent to that present in the cumulus chromite is subtracted from whole rock and recalculated to the original total before plotting. The data for Waterfall Gorge from Lightfoot and Naldrett (1984) do not include Cr and so this correction is not possible for their data. The magnitudes of these corrections can be seen in Figure 5.

Sulphides are also present in the basal olivine gabbro and picrite at Waterfall Gorge (Lightfoot and Naldrett, 1984) and their abundance indicates that they too are a cumulus component. Copper values in excess of 100 ppm are assumed to represent cumulus sulphide, which has a composition of 5% Cu and 50% Fe (Lightfoot et al., 1984). An amount of FeO proportional to the amount of Cu in excess of 100ppm in the whole rock is subtracted from the analysis to exclude the effect of sulphide accumulation. The analysis is recalculated to the original total for plotting. This is only significant for the data from Waterfall Gorge, as all other profiles are essentially barren of sulphide (c.f. Cu contents in Table 1).

The effects of the presence of sulphide and chromite can be seen to be relatively small and have little effect on the subsequent discussion.

A. Primary Olivine Compositions

The most convincing linear trend of whole rock analyses is obtained for the Waterfall Gorge section as it displays the greatest range of MgO contents. A common line is plotted on all the diagrams to show that the

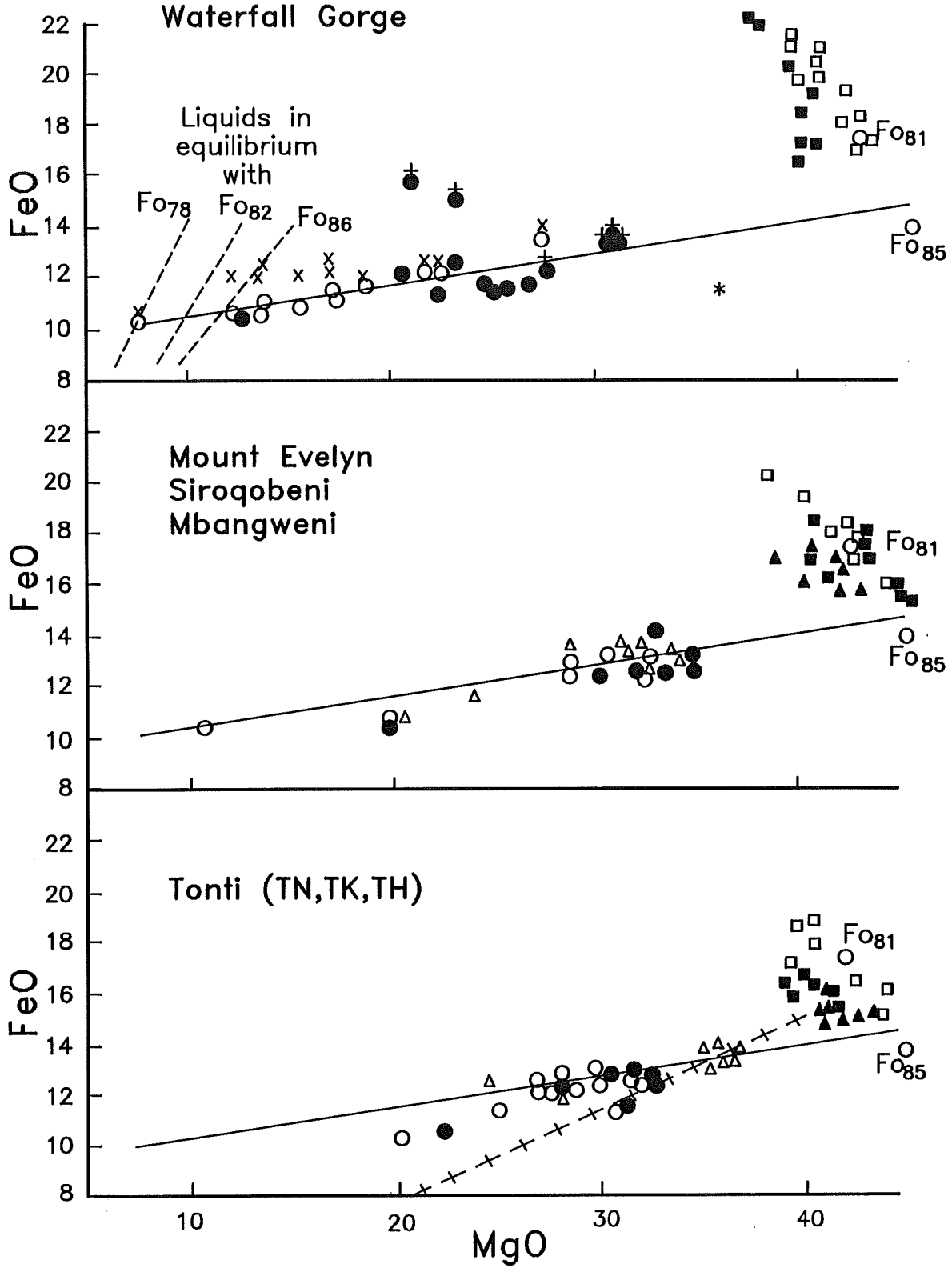

Figure 5: MgO versus FeO variation diagrams for all profiles through the Mount Ayliff Intrusion. The composition of Fo_{85} and Fo_{81} are shown as circles for reference. Compare this diagram with Figure 1. The top diagram shows all the data for the Waterfall Gorge section. Crosses are the raw data from Lightfoot and Naldrett (1984), while the open circles show the same analyses corrected for Fe in sulphide. Solid circles show the analyses (this study) recalculated with Fe in chromite removed. A few original analyses are shown as pluses to illustrate the magnitude of this recalculation. Star is from Eales (1980), open squares are olivine analyses from Lightfoot et al. (1984) by electron microprobe, and solid squares are from this study by XRF analysis on mineral separates.

data for all profiles are broadly similar. One sample analysed by Eales (1980) from a borehole drilled 20 km northeast of Waterfall Gorge is included and is distinctly lower in FeO. This may suggest that there is a different parental magma involved in the formation of this section.

It is apparent that the compositions of the olivine obtained both by electron microprobe and XRF are distinctly enriched in iron compared to that predicted by the linear relationship displayed by the whole rock data. In Figure 5 the data for Waterfall Gorge of Lightfoot and Naldrett (1984) are slightly enriched in FeO compared to the present data, which is partially but not wholly, due to the fact that Cr is not quoted and so no correction for chromite can be applied. The trends in Figure 5 indicate that the cumulus olivine composition is in the range Fo_{84-86}.

B. Magnitude of Trapped Liquid Shift

The actual analysed olivine compositions range from Fo_{77-83}, and so cannot represent the primary compositions. There can be little doubt that the trapped liquid shift has rotated the tie-lines between olivine and residual liquid during postcumulus crystallization to produce the observed spread of olivine compositions (Fig. 5).

The magnitude of this trapped liquid shift can be assessed by examining the proportion of olivine in relation to its composition. As discussed by Barnes (1986) and illustrated in Figure 1, the greater the proportion of olivine the smaller the effect on the olivine composition should be. The parallel trends for Zr in whole rock and Fo in olivine in Figure 4 demonstrate that the smaller the proportion of olivine (and hence higher Zr content in the whole rock) the more Fe-rich the olivine.

The normative proportion of olivine in the whole rock is plotted against analysed Fo content (Fig. 6), and shows an extremely good correlation, consistent with the predictions of Barnes (1986). Extrapolating to 100% olivine will define the composition of the primary olivine. This lies in excess of Fo_{86}, and so is comparable to or slightly higher than predicted by Figure 5. Eales (1980) also concluded, on the basis of chemical variation, that the primary composition of olivine in this intrusion was Fo_{86}.

C. Trapped Versus Migrating Interstitial Liquid

The calculations of Barnes (1986) depend upon the interstitial liquid being trapped. If the interstitial liquid is free to migrate then the extent of reaction cannot be predicted. For example, there could have been channelways within the crystal mush along which relatively large volumes of liquid migrated, having a major effect on the cumulus mineral compositions, even though the final apparent porosity of that rock need not be particularly high. If this had happened on a significant scale there would be a very poor correlation in Figures 4 and 6. The fact that it is tightly constrained suggests that liquid migration has been minimal. Eales (1980) recorded one isolated sample of picrite anomalously enriched in certain incompatible elements which he attributed to local enrichment in interstitial liquid, indicating that such processes may occasionally occur and are recognisable from trace element analysis.

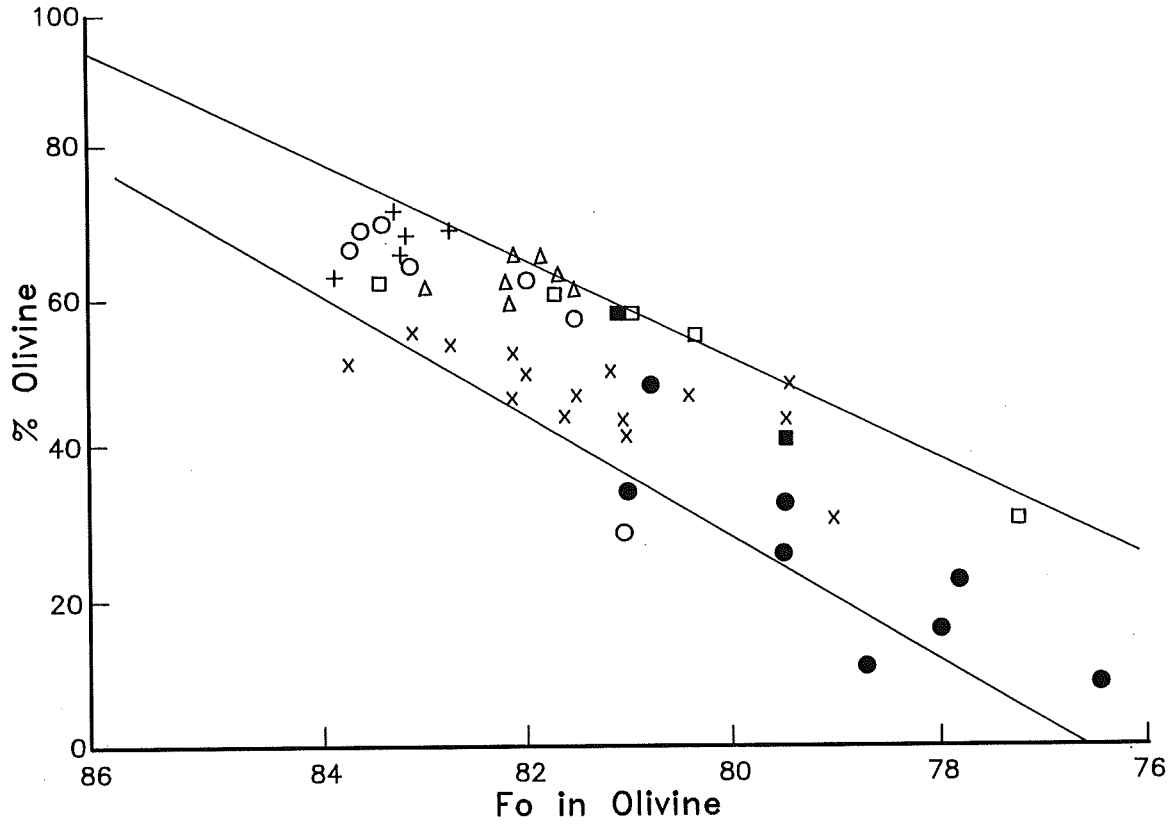

Figure 6: Plot of Fo content in olivine versus normative proportion of olivine in bulk rock. This shows that the greater the proportion of olivine in the rock the smaller the change in olivine composition from its presumed primary composition of Fo_{86}*, as predicted by Figure 1. Where olivine is scarce, samples show a shift in composition of up to 9 mole% Fo. All the samples define a fairly restricted trend. If there had been migration rather than trapping of residual liquid, greater scatter of the data would be expected. Symbols: solid circles - Waterfall Gorge; open circles - Mount Evelyn; open squares - TH; triangles - TN; pluses - TK; crosses - Mbangweni; solid squares - Siroqobeni.*

D. Differentiation

The above discussions have assumed that the primary composition of the olivine was constant in all the samples, and that all the variation observed is due to trapped liquid shift. This is probably an over-simplification of reality. However, if there is normal vertical differentiation in the primary olivine compositions, it would mean that the trapped liquid shift had been even more effective in the lowermost rocks. Differentiation and trapped liquid shift effects can be compared in a plot of Fo versus Ni content of olivine (Fig. 7). Barnes (1986) calculated how these should be related during magmatic fractionation. The compositions of primary olivine are shown by the trend marked "adcumulate" in Figure 7,

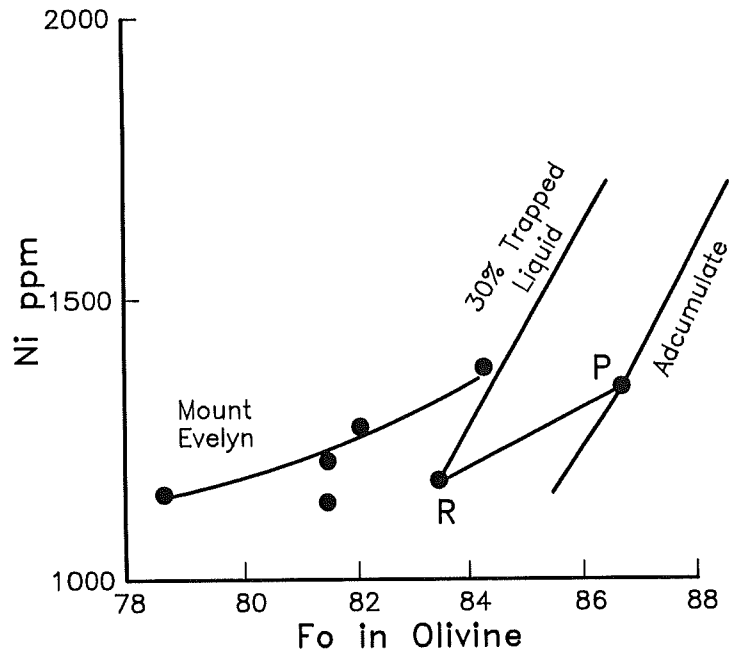

Figure 7: Plot of Ni in ppm in olivine versus forsterite content of olivine, for Mount Evelyn profile. "Adcumulate" and "30% trapped liquid" trends are taken from Barnes (1986), and refer to calculated compositions of primary olivine and the change due to trapped liquid shift. Points P and R refer to specific primary and re-equilibrated olivine demonstrating direction of trapped liquid shift.

indicating that if they formed a true adcumulate rock these would be the preserved compositions. Formation of a mesocumulate rock would permit changes in the olivine composition by trapped liquid shift to those marked "30% trapped liquid". The change for a specific olivine composition is shown by the line from P (primary mineral) to R (re-equilibrated mineral). The data for the Mount Evelyn profile are included in Figure 7 and parallel the trend PR. This suggests that the variation in compositions could be explained by changes in the proportion of trapped liquid, but starting with a slightly different parental composition from that used by Barnes (1986). Differentiation would produce a trend parallel to the "adcumulate" or "30% trapped liquid" curves, which is not observed in the data. Hence, it would appear that the extent of differentiation is not significant in relation to the effect of trapped liquid shift.

E. Parental Magmas

The range of liquid compositions in equilibrium with olivine Fo_{84-86} can be determined from the equations of Roeder and Emslie (1970), and is plotted in Figure 5. The intersection of these liquid trends with the bulk rock trends constrains the composition of the parental magma. If the primary olivine is Fo_{86}, the parental magma must contain 10.8% MgO and 10.5% total FeO. It is important to note that if a trend is extrapolated from the cluster of olivine compositions through the cluster of whole rock compositions for profiles TH, TN and TK, an apparent parent magma would be inferred which is extremely depleted in FeO (4.5% FeO at 5% MgO). From the above discussion it can be inferred that this represents the composition of the residual liquid as it re-equilibrates with the olivine, and is not the parental magma.

F. Rates of Re-equilibration

In this study and the more extended vertical profiles of Cawthorn et al. (1986) and Lightfoot et al. (1984) the writers note that the reverse trend extends over an interval of at least 60m in the Mount Evelyn profile and 20-30m at Waterfall Gorge). Above this height the proportion of olivine to trapped liquid becomes constant at about 80:20 (Eales, 1980), and so the magnitude of the trapped liquid shift is constant. The most iron-rich olivines occur near the base of the profiles, suggesting that they have undergone the greatest degree of trapped liquid shift (Fig. 4). It is difficult to calculate how long these marginal samples took to cool and crystallize from their liquidus to solidus temperatures, thereby, defining the time available for the trapped liquid shift to occur and how much liquid would be available for reaction. However, compared to most layered complexes it would have been extremely short, and yet the trapped liquid shift process seems to have been effective. If a sample 1m from the lower contact (Fig. 4) has its olivine composition reset by up to 9 mole% Fo, almost every intrusive and even some extrusive minerals must have been influenced by the trapped liquid shift.

G. Comparison with Stillwater Complex

Raedeke and McCallum (1984) reported a similar reverse differentiation trend for 400m above the base of the Stillwater Complex, and suggested that it resulted from this same process. Unfortunately, they do not give any whole rock analyses to provide independent evidence for the variation in proportion of trapped liquid through this section, but if these variations are the result of the trapped liquid shift it implies a far more gradual change in interstitial liquid content than observed in the Mount Ayliff Intrusion.

CONCLUSIONS

An independent test for the trapped liquid shift of Barnes (1986) is presented. This test is possible solely because a suite of rocks has been sampled which display a wide range of cumulus to liquid proportions within a short vertical interval. It is aided by the fact that there is only one major cumulus silicate phase - olivine. Whole rock analyses from the picritic rocks of the Mount Ayliff Intrusion define a linear trend, which can be extrapolated to constrain the composition of the primary cumulus olivine (Fo_{84-86}). This primary composition differs markedly from the compositions observed in the same rocks (Fo_{77-83}), verifying the trapped liquid shift hypothesis. The extent of the shift in composition is directly related to the proportion of interstitial liquid; a consequence of the trapped liquid shift model, as distinct from models which permit residual liquid to migrate vertically.

As a result of the rotation of tie-lines in oxide binary diagrams due to the trapped liquid shift an incautious or poorly constrained interpretation of a suite of cumulates and their observed cumulus composition could yield an erroneous inferred parental liquid composition.

ACKNOWLEDGEMENTS

Logistical support in southern Tonti to IMJ was generously provided by Johannesburg Consolidated Investments Co. Ltd. Financial support to RGC and BKS from the Foundation for Research and Development (South Africa) is gratefully acknowledged. Drs S.J. Barnes and F.J. Kruger reviewed an earlier draft of this manuscript. Geochemical, drafting, photographic and secretarial assistance was provided by Ms. N. Day, Ms. L. Whitfield, Mr. M. Hudson, Ms. J. Wilmot and Mrs. J. Long.

REFERENCES

Barnes, S.J. (1986). The effect of trapped liquid crystallization on cumulus mineral compositions in layered intrusions. Contrib. Mineral. Petrol., 93, 524-531.

Cawthorn, R.G., Groves, D.I. and Marchant, T. (1985). Magnesian ilmenite: clue to high-Mg parental magma of the Insizwa Intrusion, Transkei. Can. Mineral., 23, 609-618.

Cawthorn, R.G., De Wet, M., Maske, S., Groves, D.I. and Cassidy K.F. (1986). Nickel sulphide potential of the Mount Ayliff Intrusion (Insizwa Complex) Transkei. S. Afr. J. Sci., 82, 572-576.

Cawthorn, R.G., Maske, S., De Wet, M., Groves, D.I. and Cassidy K.F. (1988). Contrasting magma types in the Mount Ayliff Intrusion (Insizwa Complex), Transkei: evidence from ilmenite compositions. Can. Mineral., 26, 145-160.

Cawthorn, R.G., De Wet, M., Hatton, C.J. and Cassidy K.F. (1991). Titanium-rich chromite from the Mount Ayliff Intrusion: further evidence for high titanium tholeiitic magma. Amer. Mineral., 76, 561-573.

Chalokwu, C.I. and Grant, N.K. (1987). Re-equilibration of olivine with trapped liquid in the Duluth Complex, Minnesota. Geology, 15, 71-74.

Donaldson, C.H. (1976). An experimental investigation of olivine morphology. Contrib. Mineral. Petrol., 57, 187-213.

Eales, H.V. (1980). Contrasted trace-element variations in two Karroo cumulus complexes. Chem. Geol., 29, 39-48.

Irvine, T.N. (1978). Infiltration metasomatism, adcumulus growth, and secondary differentiation in the Muskox Intrusion. Carnegie Inst. Washington Yrbk., 77, 743-751.

Irvine, T.N. (1980). Magmatic infiltration metasomatism, double-diffusive fractional crystallization, and adcumulus growth in the Muskox Intrusion and other layered intrusions. In: Hargraves, R.B., (Ed.), Physics of Magmatic Processes, Princeton University Press, New Jersey, 326-383.

Lightfoot, P.C. and Naldrett, A.J. (1984). Chemical variation in the Insizwa Complex, Transkei, and the nature of the parent magma. Can. Mineral., 22, 111-123.

Lightfoot, P.C., Naldrett, A.J. and Hawkesworth C.J. (1984). The geology and geochemistry of the Waterfall Gorge section of the Insizwa Complex with particular reference to the origin of the nickel sulfide deposits. Econ. Geol., 79, 1857-1879.

Lightfoot, P.C., Naldrett, A.J. and Hawkesworth C.H. (1987). Re-evaluation of chemical variation in the Insizwa Complex, Transkei. Can. Mineral., 25, 79-90.

Lofgren, G.E. (1980). Experimental studies on the dynamic crystallization of silicate melts. In: Hargraves, R.B. (Ed.), Physics of Magmatic Processes, Princeton University Press, New Jersey, 487-551.

Paktunc, A.D. (1987). Differentiation of the Cuthbert Lake ultramafic dykes and related mafic dykes. Contrib. Mineral. Petrol., 97, 405-416.

Raedeke, L.D. and McCallum, I.S. (1984). Investigations in the Stillwater Complex: Part II. Petrology and petrogenesis of the ultramafic series. J. Petrol., 25, 395-420.

Roeder, P.L. and Emslie, R.F. (1970). Olivine-liquid equilibrium. Contrib. Mineral. Petrol., 29, 275-289.

Scholtz, D.L. (1936). The nickeliferous ore deposits of East Griqualand and Pondoland. Trans. geol. Soc. S. Afr., 39, 81-210.

Tait, S.R., Huppert, H.E. and Sparks, R.S.J. (1984). The role of compositional convection in the formation of adcumulate rocks. Lithos, 17, 139-146.

Walker, D., Kirkpatrick, R.J., Longhi, J. and Hays J.F. (1976). Crystallization history of lunar picrite basalt sample 12002: phase equilibria and cooling rate studies. Geol. Soc. Amer. Bull., 87, 646-656.

Wilson, J.R., Menuge, J.F., Pedersen, S. and Engell-Sorensen, O. (1987). The Southern part of the Fongen-Hyllingen layered mafic complex, Norway: emplacement and crystallization of compositionally zoned magma. In: Parsons, I. (Ed.), Origins of Igneous Layering, Reidel, Dordrecht, (NATO ASI Series C, No. 196), 145-184.

oOo